

# Cubic GaN/AlN multi-quantum wells grown on pre-patterned 3C-SiC/Si (001)

R. M. Kemper<sup>1,2</sup>, C. Mietze<sup>1,2</sup>, L. Hiller<sup>3</sup>, T. Stauden<sup>3</sup>, J. Pezoldt<sup>3</sup>, D. Meertens<sup>4</sup>, M. Luysberg<sup>4</sup>, D. J. As<sup>1,2</sup>, and J. K. N. Lindner<sup>1,2</sup>

<sup>1</sup>University of Paderborn, Department of Physics, Warburger Str. 100, 33098 Paderborn, Germany

<sup>2</sup>Center for Optoelectronics and Photonics, Warburger Str. 100, 33098 Paderborn, Germany

<sup>3</sup>FG Nanotechnologie, Institut für Mikro- und Nanotechnologien MacroNano<sup>®</sup>, Technische Universität Ilmenau, Postfach 100565, 98684 Ilmenau, Germany

<sup>4</sup>Ernst-Ruska Centre for Microscopy and Spectroscopy with Electrons, Forschungszentrum Jülich, 52425 Jülich, Germany

Received 27 June 2013, accepted 13 November 2013

Published online 16 January 2014

**Keywords** nitrides, molecular beam epitaxy, TEM, planar defects

\* Corresponding author: e-mail rkemper@mail.upb.de

We report for the first time on the growth of cubic AlN/GaN multi-quantum wells (MQWs) on pre-patterned 3C-SiC/Si (001) substrates. The sample structure consists of 10 periods of 2 nm c-AlN barriers with a 4 nm c-GaN layer in between, which were grown on 3C-SiC post shaped structures by means of molecular beam epitaxy. Substrate patterning has been realized by electron beam lithography and a reactive ion etching process. The 3C-

SiC posts have a length of about 550 nm and a height of about 700 nm. (Scanning) transmission electron microscopy studies show that the morphology of the MQWs is clearly influenced by {111} stacking faults, modulating the local growth rate. Further, the growth at the edges of the surface pattern is investigated. The MQW layers cover the 90° edges by developing low-index facets rather than by forming a conformal system of 90° angled layers.

© 2014 WILEY-VCH Verlag GmbH & Co. KGaA, Weinheim

**1 Introduction** Group III-nitrides, like GaN and AlN, have great potential for novel nitride devices like quantum well infrared photodetectors and quantum cascade lasers. For the development and the design of optoelectronic intersubband devices a general understanding of multi-quantum well (MQW) growth processes and the formation of defects is of crucial importance. Presently, the growth of thin films on prepatterned surfaces attracts great attention as a method to reduce defect densities [1].

While most studies deal with hexagonal polytypes it is advantageous to use the cubic III-nitrides (like c-GaN and c-AlN), since they exhibit no inherent spontaneous and piezoelectric polarization fields in [001] growth direction, which is an important benefit for the realization of electronic devices. In the cubic system Zainal and coworkers [2] have shown resonant tunneling through cubic GaN/AlGaN double barriers on GaAs substrates. Furthermore, Mietze et al. [3] demonstrated resonant tunnel diodes with reproducible I-V characteristics and recoverable

negative differential resistance based on cubic Al(Ga)N/GaN double barrier structures on 3C-SiC (001).

The heteroepitaxial growth of c-GaN and c-AlN by molecular beam epitaxy (MBE) is possible in a narrow window of experimental conditions and with an adequate substrate [4,5]. Due to the lack of cubic GaN bulk substrates 3C-SiC (001) is the substrate of choice [6]. The lattice mismatch between the 3C-SiC substrate and c-GaN is about 3.5% and is meant to be the main reason for the formation of defects. High-resolution X-ray diffraction measurements have shown that the dislocation density of c-GaN deposited on 3C-SiC (001) by plasma assisted MBE is in the order of magnitude of  $10^{10}$ - $10^{11}$  cm<sup>-2</sup> [7]. In contrast, the mismatch between 3C-SiC and c-AlN is just about 0.25% leading to a slightly lower dislocation density of about  $8 \times 10^9$  cm<sup>-2</sup> [4]. Thus, the first approach towards defect reduction in c-GaN should be to start the MQW growth with c-AlN layers.

In this work, we investigate the structural quality of non-polar c-AlN/GaN MQWs on pre-patterned 3C-SiC/Si (001) substrates by MBE. The growth of such a layer system on a prepatterned surface gives us the opportunity to study both the influence of defects on layer growth and the observation of the growth behaviour at edges of the surface pattern.

**2 Experimental** The substrates consist of 12  $\mu\text{m}$  thick 3C-SiC (001) films deposited by low-pressure chemical vapor deposition [8] on top of 500  $\mu\text{m}$  Si. Patterning of the substrate surface was realized by electron beam lithography followed by reactive ion etching [9]. The surface pattern consists of posts with edges aligned parallel to the  $\langle 110 \rangle$  directions with a length of about 550 nm and a height of ca. 700 nm. After processing the patterned surface was cleaned with a buffered oxide etching solution ( $\text{NH}_4\text{F}:\text{H}_2\text{O}:\text{HF}=4:6:1$ ). On these patterned substrates 10 periods of 2 nm c-AlN barriers with a 4 nm c-GaN layer in between were grown by plasma assisted MBE. Figure 1 displays a schematic drawing of the sample structure.

Reflection high energy electron diffraction (RHEED) was used to monitor *in-situ* the crystalline nature and morphology of the sample surface. The growth temperature was 720°C. The c-AlN was grown under 1 ML Al coverage at the substrate surface [4] and the c-GaN layers were grown under Ga-rich conditions with 1 ML Ga coverage at the surface [5]. After growth the structural quality of the samples was studied by (scanning) transmission electron microscopy (S)TEM. For cross-section TEM measurements the samples were prepared using a focussed ion beam. For this the posts were first covered with two thick platinum protection layers and then the TEM lamellae were cut through a row of posts parallel to the [110] direction. STEM investigations were performed with a  $C_s$  probe corrected FEI Titan microscope operated at 300 kV.

**3 Results and discussion** Figure 2 shows a side view scanning electron microscopy (SEM) image of an  $5 \times 5$  array of 3C-SiC posts overgrown with the MQW film. The sidewalls of the posts have a varying steepness. At the bottom the posts are surrounded by trenches due to the etching process [9]. Film deposition takes place on the top, on the sidewalls and between the posts. The whole patterned area is covered with the MQW film. In between neighbouring posts deepenings in the layer are seen. They are probably due to shadowing in particular when the rotation of the sample holder is stopped during MBE growth for RHEED inspection of the growth surface.

Figure 3 displays a cross-sectional TEM image of an individual 3C-SiC post overgrown with 10 periods of c-AlN/GaN MQWs taken along the [110] zone axis. The post is covered by the two Pt layers due to the TEM specimen preparation. The post has slightly curved sidewalls. V-groove trenches are formed at the bottom of the post. The top of the post and also the sidewalls as well as the free surface in between are covered with the MQW film.

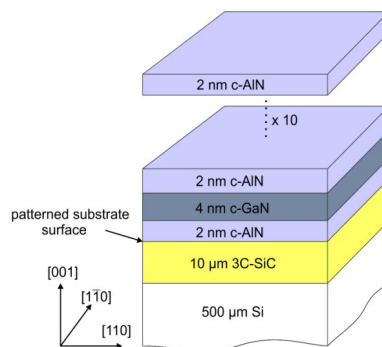


**Figure 1** Schematic drawing of the sample structure.

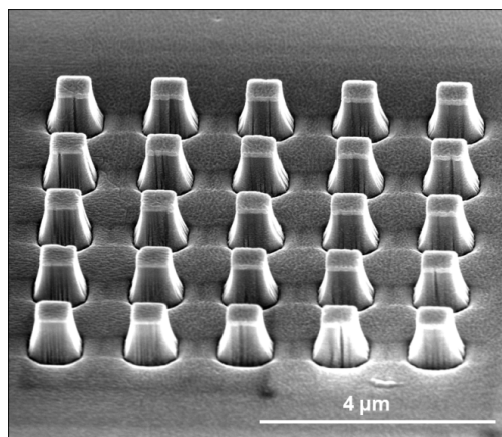


**Figure 2** Side view SEM image of an array of overgrown 3C-SiC (001) posts.

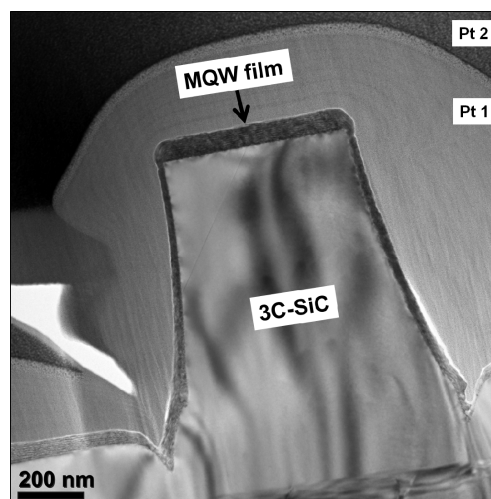


**Figure 3** Cross-sectional TEM bright-field image of an individual 3C-SiC post overgrown with 10 periods of c-AlN/GaN MQWs taken along the [110] zone axis.

It should be noted that all posts exhibit almost identical growth morphologies of the MQW film and a surprisingly identical internal defect distribution.

Figure 4(a) shows a more detailed bright-field TEM image of the MQW film on top of the 3C-SiC post in Fig. 3. Due to the difference in electron extinction lengths the

c-GaN layers (dark) and the c-AlN barriers (bright) can be clearly separated. Figure 4(a) shows bunches of  $\{111\}$  stacking faults propagating through the entire MQW layer stack. The stacking faults emerge from the 3C-SiC/c-AlN interface and are not stopped at the c-GaN/AlN interfaces of the different layers. In regions with a high stacking fault density the sequential arrangement of c-AlN/GaN layers is disturbed which generates an undulating shape of the MQWs. In contrast in regions without any planar defects a planar sequential arrangement of c-AlN and c-GaN layers is observed with uniform growth rate.

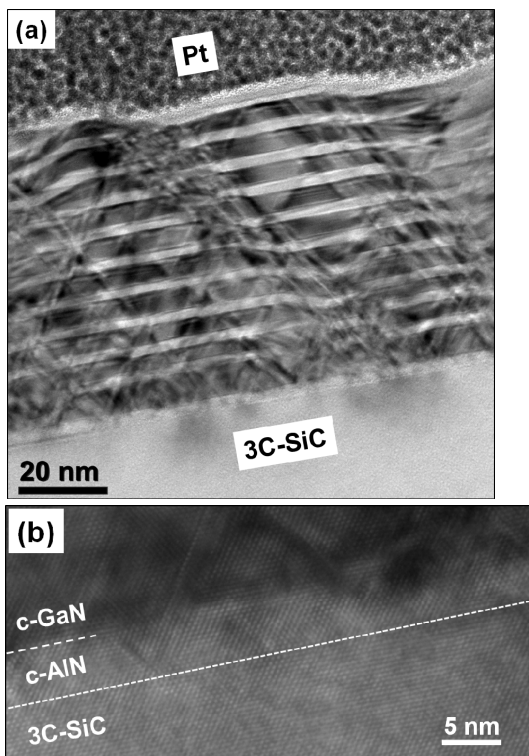


**Figure 4** (a) TEM image along the  $[110]$  zone axis of the MQWs on top of the 3C-SiC post. In regions with a high stacking fault density the sequential arrangement of the MQWs is disturbed. (b) High-resolution TEM image along the  $[110]$  zone axis of the 3C-SiC/c-AlN interface on top of the post.

Strong undulations may occur right within the first few layers of the MQW stack. In some cases these undulations are transferred up to the surface, leading to surface hillocks. In other cases these undulations are smoothed in subsequent layers, leading to a smooth surface at the top. Care must be taken therefore if one would try to judge the smoothness of MQW layer stacks from measurements of the surface smoothness of a layer stack (using SEM or scanning probe techniques). It should be emphasized that undulations generated in the first few layers on the substrate are not transferred vertically towards the surface but follow the propagation of the stacking faults, indicating a locally reduced growth rate around the stacking faults.

The stacking faults arise although the misfit between the 3C-SiC substrate and the first c-AlN layer is small. To understand the growth process of the first c-AlN layer a high-resolution TEM image of the interface of the 3C-SiC substrate and the c-AlN is shown in Fig. 4(b). It is observed that the c-AlN/3C-SiC interface is atomically smooth and exhibits an undisturbed crystalline structure. The first c-AlN layer has an average thickness of 6 ML and a comparatively rough, three-dimensional interface to the c-GaN film on top. One explanation for this tendency to island formation can be the difference in surface energies of the 3C-SiC substrate and the c-AlN as described in detail in Ref. [4]. It is reported that after 6 ML c-AlN growth a roughness transition of the surface from 2D into 3D-islands is observed. After a growth of 10–20 ML the surface transforms back into a smooth 2D state. This transformation depends on the Al coverage of the growth front [4]. It is obvious that optimized growth conditions of the first c-AlN layer are essential to improve the MQW growth. The growth of the following (first) c-GaN layer is affected by the rough surface and the lattice mismatch with the first c-AlN layer. These may be the main reasons for the formation of  $\{111\}$  stacking faults with a  $54.7^\circ$  slope towards the surface which occur at a high density in this layer and all layers on top, frequently forming bunches of planar defects. The density of planar defects seems to be largest within the first c-GaN layer (Fig. 4(a)) but is similar in the AlN layer underneath. This might indicate that the stacking faults nucleate at the c-AlN/GaN interface and then extend into both, the c-GaN and the c-AlN film underneath.

Occasionally it is also observed that stacking faults originating from the 3C-SiC substrate are extended into the MQW film. However, since the density of stacking faults in the 3C-SiC substrate is comparatively small this mechanism plays a minor role for the stacking fault formation in the MQW layer stack.

Due to the contrast between c-AlN and c-GaN layers in STEM images the MQW structure investigated here provides an indication of the general growth kinetics on patterned substrates. The individual MQW layers can be regarded as “annual rings” which give information about the growth behaviour especially around the edges of the posts. Figure 5(a) displays a high-angle annular dark field (HAADF) STEM image of a part of the MQW film grown on top of a 3C-SiC post and on the sidewall. In the HAADF-STEM modus the contrasts are less influenced by local strains and atomic columns appear as bright dots with the intensity increasing with increasing atomic number. Therefore, GaN layers can be distinguished from AlN by their higher intensity, i.e. the contrasts are inverted with respect to TEM images in Fig. 4. The MQW film on top of the post in  $[001]$  growth direction encloses the almost perfectly rectangular edge of the post. Judging from the progress of the individual layers it looks like the MQW film is bent around the 3C-SiC edge. Further, the growth on the  $(001)$  plane is not influenced by the growth on the sidewall of the post. The inset in Fig. 5(a) displays an enlarged sec-

tion of the overgrown post edge with indexed facets. It is obvious that the MQW layers cover the (nearly) 90° edge by developing low-index facets rather than by forming a conformal system of 90° angled layers. Most pronounced is a (111) facet, which – in each layer – ends directly above the 90° edge of the 3C-SiC post.

In Fig. 5(b) a TEM bright-field image along the [110] zone axis of the MQW film around the 3C-SiC post-edge is shown. A bunch of {111} stacking faults occurs directly at the edge. In this area (the beginning is marked with a dashed line in Fig. 5(b)) the individual MQWs are bent parallel to the {111} stacking faults and the growth

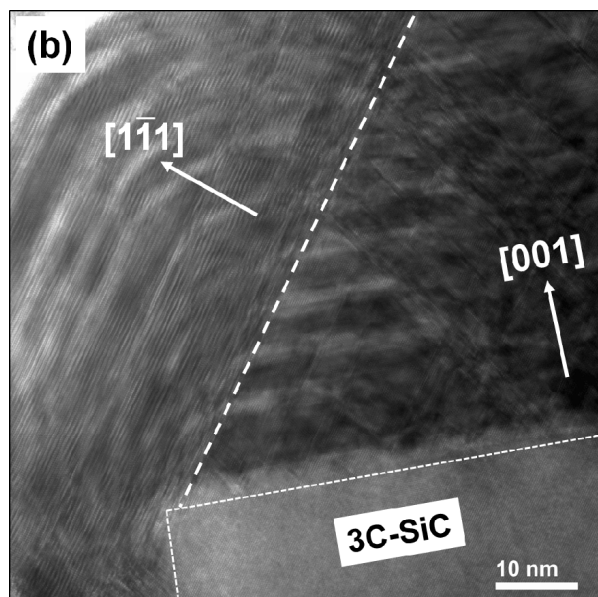
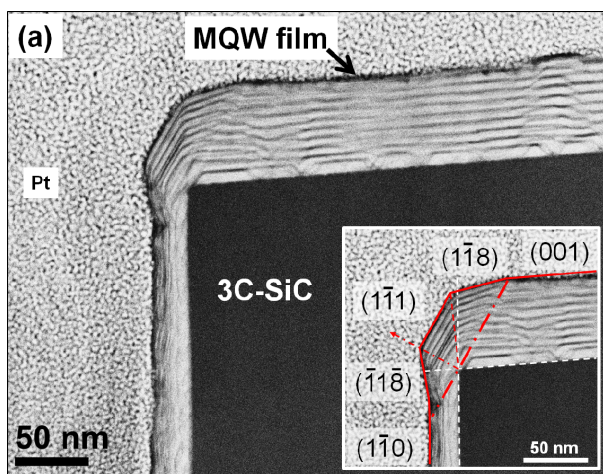


**Figure 5** (a) STEM image along the [110] zone axis of a part of the MQW film grown on top of a 3C-SiC post and around the edge. Inset: the MQW layers cover the (nearly) 90° edge by developing low-index facets. (b) TEM bright-field image along the [110] zone axis of the MQW film around the 3C-SiC post edge. At the edge the individual MQWs are bent parallel to the {111} stacking faults. The diffuse contrast results from the high stacking fault density.

direction is changed to the [111] direction. Additionally the thickness of the individual MQW layers is varying compared to the growth in [001] growth direction indicating a different growth rate in this region. Here the crystalline nature is dominated by stacking faults which promotes the hexagonal phase. In fact, Fourier transformed images (not shown) of the region above the (111) facet give a hexagonal rather than a cubic reciprocal lattice. The diffuse contrasts in this region result from the high defect density. So far it is not clear whether the shape of the substrate edge influences the formation of stacking faults. The investigation of the detailed growth kinetics especially on substrate edges are subject of further studies.

**4 Conclusions** In summary, we have shown that it is possible to grow cubic AlN/GaN MQWs on pre-patterned 3C-SiC substrates by means of MBE. {111} stacking faults occur and continue through the entire layer stack and generate regions with locally reduced growth rate. This leads to an undulating shape of the MQW film. The stacking faults are mainly induced by the three-dimensional morphology of the first layers on the SiC substrate. Therefore, any major improvements of the MQW morphology can be achieved only by eliminating the island growth of these initial layers. It is shown that MQW films do not grow conformally around (nearly) 90° SiC edges along <110> directions, but form {111} facets which promote the formation of hexagonal inclusions in both, the c-GaN and the c-AlN films.

**Acknowledgements** The authors would like to thank Dr. András Kovács from the Ernst-Ruska Centre for Microscopy and Spectroscopy with Electrons, Forschungszentrum Jülich, for TEM sample preparation.

## References

- [1] R. M. Kemper, L. Hiller, T. Stauden, J. Pezoldt, K. Duschik, T. Niendorf, H. J. Maier, D. Meertens, K. Tillmann, D. J. As and J. K. N. Lindner, *J. Cryst. Growth*, doi: 10.1016/j.jcrysgro.2012.10.011 (2012).
- [2] N. Zainal, S. V. Novikov, C. J. Mellor, C. T. Foxon, and A. J. Kent, *Appl. Phys. Lett.* **97**, 112102 (2010).
- [3] C. Mietze, K. Lischka, and D. J. As, *Phys. Status Solidi A* **209**, 439 (2012).
- [4] T. Schupp, K. Lischka, and D. J. As, *J. Cryst. Growth* **312**, 1500-1504 (2010).
- [5] J. Schörmann, S. Potthast, D. J. As, and K. Lischka, *Appl. Phys. Lett.* **90**, 041918 (2007).
- [6] S. V. Novikov, N. M. Stanton, R. P. Campion, C. T. Foxon, and A. J. Kent, *J. Cryst. Growth* **310**, 3964 (2008).
- [7] P. Gay, P. B. Hirsch, and A. Kelly, *Acta Metall.* **1**, 315 (1953).
- [8] T. Chassagne, A. Leycuras, C. Balloud, P. Arcade, H. Peyre, and S. Juillaguet, *Mater. Sci. Forum* **457-460**, 273-276 (2004).
- [9] L. Hiller, T. Stauden, R. M. Kemper, J. K. N. Lindner, D. J. As, and J. Pezoldt, *Proc. Mater. Sci. Forum* **717-720**, 901 (2012).